Hydrology Research

Hydrology Research Vol 55 No 3, 263 doi: 10.2166/nh.2024.059

Estimating groundwater recharge rates in the Upper Awash Basin, Ethiopia under different combinations of model complexity and objective functions

Muauz Amare Redda[a,*], Seifu Kebede[b], Behailu Birhanu[c] and Bediru Hussien[d]

[a] Ethiopian Institute of Water Resource, Addis Ababa University, Addis Ababa, Ethiopia
[b] Center for Water Resources Research, School of Agricultural Earth and Environmental Sciences, University of KwaZulu Natal, Pietermaritzburg 3201, South Africa
[c] School of Earth Sciences, Addis Ababa University, Addis Ababa, Ethiopia
[d] School of Earth Sciences and Engineering, Addis Ababa Science and Technology University, Addis Ababa, Ethiopia
*Corresponding author. E-mail: muauzamare@yahoo.com

ABSTRACT

This study addresses the critical need for reliable groundwater recharge quantification by investigating the uncertainty associated with recharge estimation based on various combinations of model complexity and objective functions. Focusing on the Hombele catchment in the upper Awash Basin, Ethiopia, the research aims to analyze parameter sensitivity under different model complexities and objectives while estimating groundwater recharge for the period 1986–2013. Employing a Monte-Carlo-based calibration scheme, the study fine-tunes model parameters using objective functions like KGE, NSE, LogNSE, R2, and VE across 10 combinations of model complexity and objective functions. Results identify FC, LP, and BETA as highly sensitive parameters, while UZL, K0, and MAXBAS show limited influence in all model complexity and objective function scenarios. The semi-distributed HBV-light model achieves calibration, validation, and overall period KGE (NSE) values of 0.89 (0.80), 0.80 (0.73), and 0.87 (0.77), respectively. Sensitivity analyses reveal significant impacts on model parameters and recharge estimation based on the chosen objective function and model complexity levels. Average annual recharge rates range from 185.9–280.5 mm when the HBV-light model is semi-distributed, contrasting with 185.3–321.7 mm under lumped model conditions, emphasizing the importance of considering these factors in groundwater resource assessments.

Key words: groundwater recharge, HBV-light model, model complexity, objective functions

HIGHLIGHTS

- Groundwater recharge rate estimation was performed using lumped and semi-distributed, conceptual hydrological HBV-light models in the upper Awash subbasin.
- Assessment model objective functions and model complexities have a significant impact on the sensitivity of the HBV-light model parameters and objective functions.
- Groundwater recharge rate was evaluated using five objective functions and five evaluation matrices.

1. INTRODUCTION

Groundwater recharge is a key component of the water balance, and as a result, accurate quantification of the rate of natural groundwater recharge is essential for sustainable groundwater resource management. The total groundwater resource in Africa is estimated to be 0.66 million km^3 (MacDonald *et al.* 2021), and this resource is unevenly distributed in the continent with the largest groundwater volumes found in North African countries such as Libya, Algeria, Egypt, and Sudan. Ethiopia has 30 billion cubic meters of groundwater resources (Kidanewold *et al.* 2014). This resource plays a vital role in supplying water for irrigation, drinking, and other purposes in arid and semi-arid regions of the nation. However, the increasing population and climate change lead to excessive withdrawal of groundwater in the region and pose a serious problem in sustainably utilizing groundwater resources. Therefore, accurate estimation of groundwater recharge rates is crucial for assessing water security and developing reliable groundwater resource management plans.

The volume of rainwater that reaches the water table cannot be immediately and reliably measured, making it difficult to estimate groundwater recharge rates (Scanlon *et al.* 2002). There are several ways to measure groundwater recharge rates;

however, each technique has inherent weaknesses due to various factors that affect the recharge rate, such as climate, geomorphology, litho-structural setting, and water table. Instead, several approaches are available to estimate the rate of groundwater recharge. Therefore, it is recommended to use multiple methods to estimate the recharge rate and compare the results to increase the reliability of the estimates. These approaches include the water balance approach (Baye *et al.* 2012; Azagegn 2014; Mechal *et al.* 2015; Neil 2015; Gidafie *et al.* 2016; Izady *et al.* 2017; Birhanu *et al.* 2018; Tenalem 2019; Yun *et al.* 2023), baseflow separation approach (Berehanu *et al.* 2017), water-level fluctuation approach (Healy & Cook 2002; Baye 2009), chloride mass balance (Scanlon *et al.* 2006; Dassi 2010; Azagegn 2014; Berehanu *et al.* 2017), AMBHAS_1D model (Verma *et al.* 2023), environmental trace and stable isotopes (Li *et al.* 2017; Parlov *et al.* 2019), and the Analytic Hierarchy Process model (Varouchakis *et al.* 2022). However, there is no widely applicable method available for estimating groundwater recharge rates because of the complexity of the groundwater system and the large variation of factors affecting the recharge rates. Therefore, it is recommended to use multiple methods to estimate recharge rates and compare the results to increase the reliability of the estimates.

Numerous previous studies have been undertaken to estimate groundwater recharge rates in the Upper Awash basin of Ethiopia using various approaches. For example, Baye (2009) applied a water table fluctuation approach to estimate the rate of groundwater recharge, and they found that the annual water recharge of the Upper Awash Basin is 90 mm/year. Similarly, Azagegn (2014) used the water balance approach, a different hydrologic model, to quantify groundwater recharge rates in the Upper Awash basin of Ethiopia, and they reported about 82.5 mm/year. The results of these studies, particularly the water balance approach, provide inconsistent results, and thus further studies need to be conducted in the study basin. The reason for the inconsistent results in the water balance approach may be associated with the structure of the model, the level of model complexity, and the applied objective functions.

Hydrologic models play a vital role in estimating groundwater recharge and support the well-informed decision on the sustainable management of these resources. A wide variety of hydrologic models with different mode complexities, structure, parameters, and input data are available to model the groundwater recharge rate. Given that the selection of a hydrologic model for quantifying the groundwater recharge rate has been challenging, it is important to understand the effect of different levels of model complexities and objective functions in estimating groundwater recharge rates. Therefore, the present study uses the HBV-light model to quantify the rate of groundwater recharge in the Upper Awash basin of Ethiopia under different levels of model complexities and objective functions. A total of 10 combinations of model complexities and objective functions were used for the analysis.

2. MATERIALS AND METHODS

2.1. Study area

The present study was undertaken in the Upper Awash basin, Ethiopia, which is located at 37°51′09″ E – 39°39′50″ longitude and 8°07′07″ N - 9°55′11″ latitude as shown in Figure 1. The elevation of the study area ranges from 1,579 to 3,564 m and covers an area of 11,690 km^2. The study area experiences 1,078 mm of annual rainfall on average, with minimal amounts of 865 mm in the lower basin regions and the highest amounts of 1,327 mm in the highland regions. The precipitation distribution is highly variable spatially – decreasing from the northwest to the southeast. The rainfall in the Upper Awash basin has a bimodal rainfall pattern with a primary rainy season occurring from June to September and a secondary rainy season starting in March and ending in May. These rainfall patterns are controlled by the movement of the Intertropical Convergence Zone (Seleshi & Zanke 2004). The average annual temperature is 18.6 °C, with a range of 16.4–21.8 °C. The maximum mean temperatures are observed in April and May and the lowest ones (only 5.2 °C less than the highest one) in January. The temperatures of the study area exhibit fewer spatial variations than precipitation. The methodology for the study area is outlined in Figure 2.

2.2. The HBV-light model's description

The HBV-light model (Seibert 1997) is a conceptual rainfall–runoff model modified from the first HBV model (Bergstrom 1991). There are two modifications within the modified model that correspond generally to the first version described by Bergström (2006). The first is that HBV-light v4.0.0.22 uses a 'warming-up' period during which state variables evolve from standard initial values to their correct values consistent with environmental conditions and parameter values. This is done in place of starting the simulation with some user-defined initial state values. Second, the routing parameter MAXBAS can now incorporate non-integer values (Zinko *et al.* 2005). An extra advantage of the HBV-light model is that Monte Carlo (MC) simulations are often performed to account for parameter uncertainty in model output using random

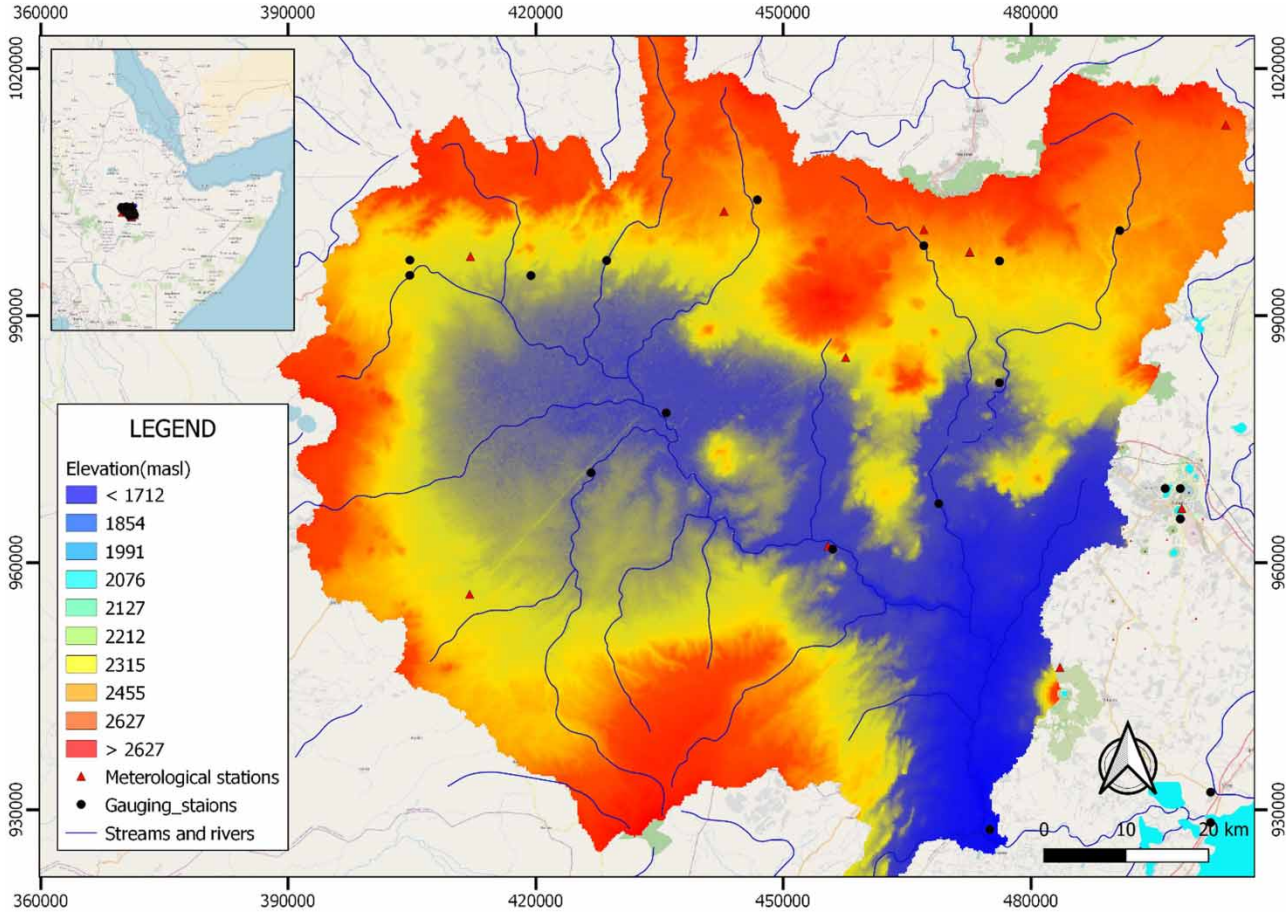

Figure 1 | Location map of the Hombele catchment.

numbers from a consistent distribution within the set ranges for every parameter. Rainfall, temperature, and potential evapotranspiration (PET) are used as inputs for simulating the streamflow. For this study area, the HBV-light model structure necessitates the parameterization of nine parameters for calibration, excluding the snow routine. However, when considering the snow routine, the model expands to encompass 14 parameters that require calibration. In general, the model is subdivided into three routines: the snow and glacier routine, the soil moisture routine, and the groundwater and response routine, as indicated in Figure 3. Table 1 describes each model parameter.

The various HBV-light model structures, concepts, and applications are described in many papers, and a comprehensive description of the model with all its equations and parameters can be found in the study by Seibert (2000). Based on the relationship between the water content of the soil box's SM (mm) and its greatest value FC (mm), rainfall (P) is divided into groundwater recharging and water filling the soil box (Equation (1)). Actual evaporation from the soil box equals the potential evaporation if SM/FC is above LP [–], while a linear reduction is used when SM/FC is below LP (Equation (2)). As part of groundwater recharge, the upper groundwater box SUZ (mm) is added. Water levels in lower lake boxes are affected by precipitation and evaporation. Water is filtered from upper to lower groundwater box at a limited rate determined by PERC. Outflow from groundwater boxes is determined by linear equations and SUZ water level reaching the UZL threshold value (Equation (3)). Runoff is calculated using a triangle weighting function from MAXBAS (Equation (4)). Finally, to provide the simulated runoff ($\Delta t - 1$, mm), this runoff is modified by a triangle weighting function provided by the parameter MAXBAS (Equation (4)).

$$\frac{\text{recharge}}{P(t)} = \left(\frac{\text{SM}(t)}{\text{FC}}\right)^{\text{BETA}} \tag{1}$$

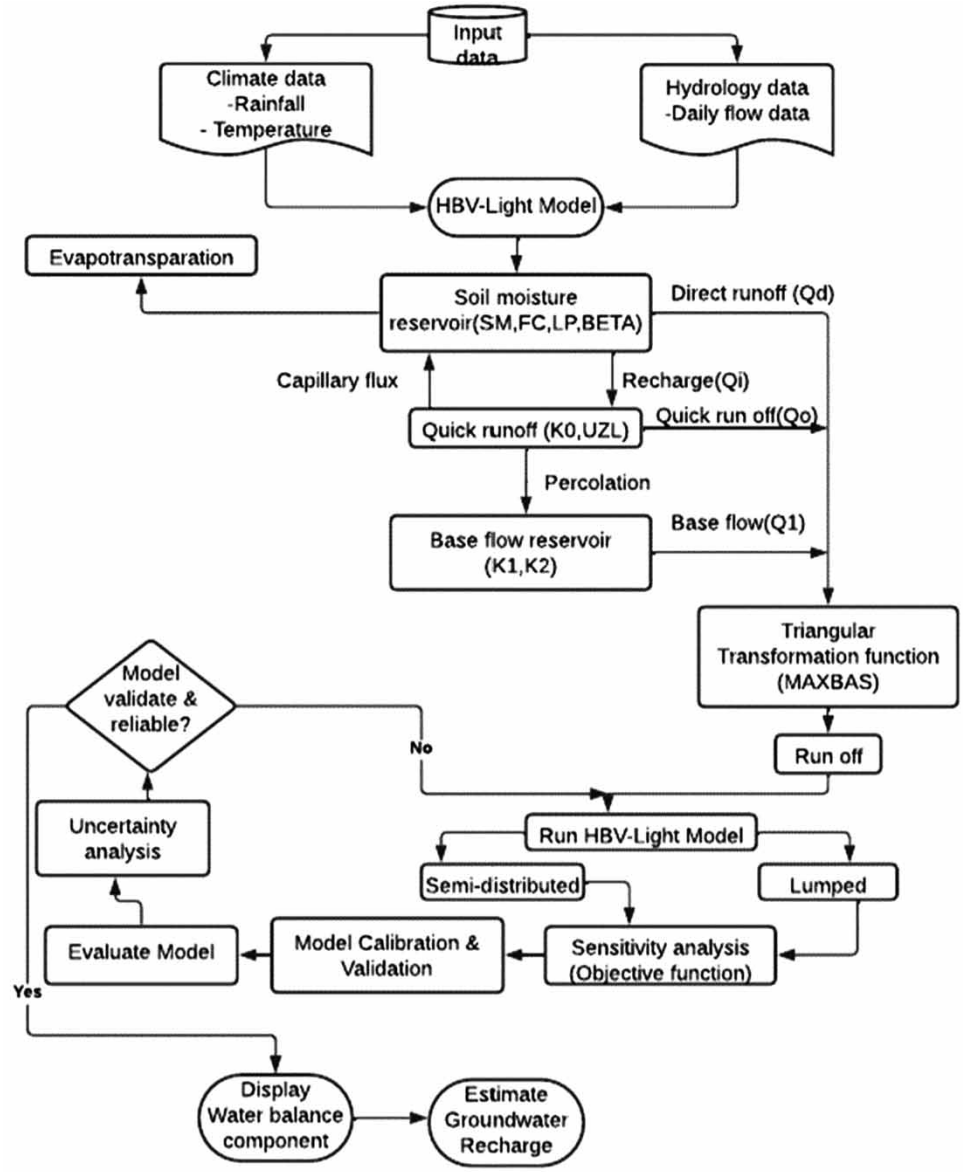

Figure 2 | Flow chart to describe the methodology.

$$E_{\text{act}} = E_{\text{pot}} \min\left(\frac{\text{SM}(t)}{\text{FC} \times \text{LP}}, 1\right) \tag{2}$$

$$Q_{\text{GW}}(t) = K_2\text{SLZ} + K_1\text{SUZ} + K_0\max(\text{SUZ} - \text{UZL}, 0) \tag{3}$$

$$Q_{\text{sim}}(t) = \sum_{I=1}^{\text{MAXBAS}} c(i) Q_{\text{GW}}(t - i + t)$$

where

$$c(i) = \int_{i-1}^{i} \frac{2}{\text{MAXBAS}} - \left|U - \frac{\text{MAXBAS}}{2}\right| \frac{4}{\text{MAXBAS}^2}\,\text{du} \tag{4}$$

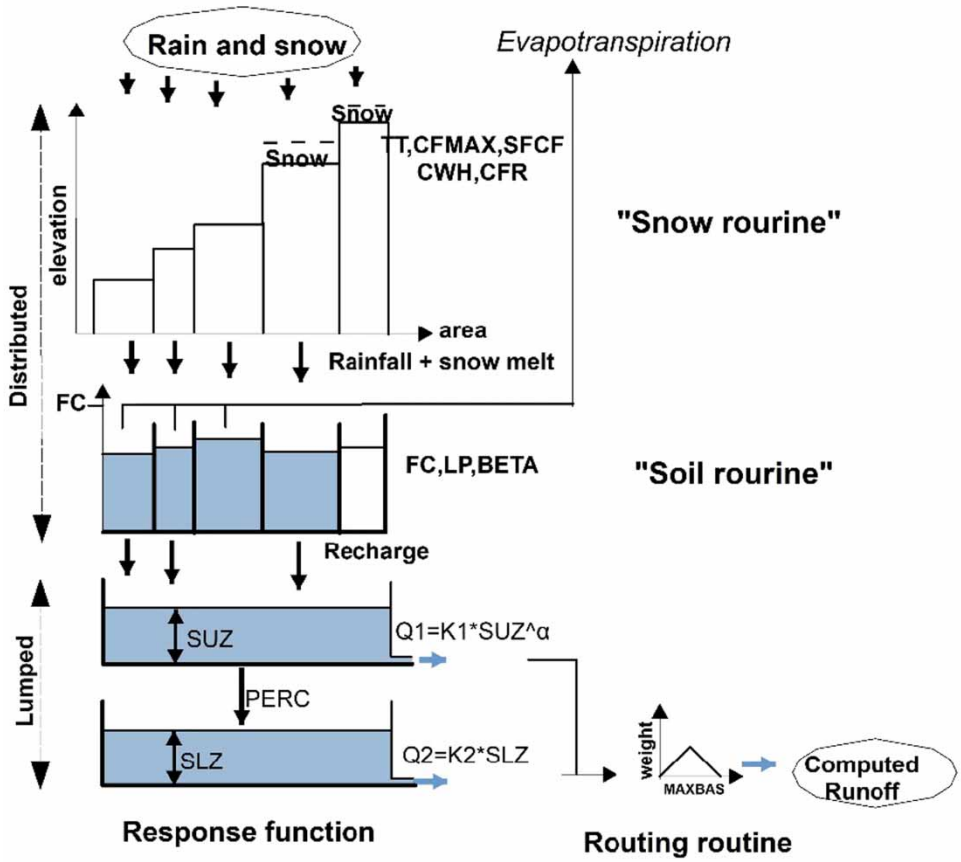

Figure 3 | The general structure of the HBV-light model (Adapted from Seibert (2000)).

Table 1 | Parameters and their ranges used for the MC simulations

Parameter	Explanation	Minimum	Maximum	Unit
Soil routine				
FC	Maximum of SM (storage in soil box)	50	500	mm
LP	Soil moisture value above which AET reaches PET	0.3	1	
BETA	Shape coefficient	1	6	
Groundwater and response routine				
K0	Recession coefficient	0.05	0.5	d^{-1}
K1	Recession coefficient	0.01	0.3	d^{-1}
K2	Recession coefficient	0.001	0.1	d^{-1}
UZL	Threshold for K0-outflow	0	100	mm
PERC	Maximal flow from upper to lower GW-box	0	6	min d^{-1}
MAXBAS	Routing, length of the weighting function	1	5	d

2.3. Dataset

The HBV-light model required input data consisting of daily precipitation and air temperature as well as monthly estimates of PET. The existing streamflow and meteorological data within the basin were obtained from the Ministry of Water, Electricity and Irrigation, and the National Metrology Agency, Government of Ethiopia, respectively. Daily streamflow data at these stations for the study period from 1986 to 2013 have been analyzed. There are altogether 14 stations with different time

records in the basin among which two have been considered. The mean monthly and annual flow of the selected gauging station is shown in Table 2 and Figure 4, respectively. The mean monthly PET was calculated from the observed meteorological data using the FAO Penman–Monteith method as reported by Allan *et al.* (1998). The mean monthly precipitation data from 14 meteorological stations from 1986 to 2013 were collected as shown in Figure 4 and Table 3, respectively. There are many methods to fill in missing data using R_package. These are interpolation, Kalman, locf, ma, mean, and Kalman method used to fill the gaps within the data series to assure data consistency and continuity. Precipitation data from the stations were used to derive a mean areal daily precipitation statistic using Thiessen polygons. Figure 3 shows the chosen meteorological and hydrological (gauge) stations. The mean monthly maximum and minimum temperatures at three selected stations for the period ranging from 1986 to 2013 are presented in Table 4. The daily temperature has been calculated as the simple average of the maximum and minimum temperatures.

Table 2 | Average monthly flow at the Hombele gauging station

Gauging station	Jan	Feb	Mar	Apr	May	Jun	Jul	Aug	Sep	Oct	Nov	Dec
Awash at Hombele	4.31	4.80	6.26	9.94	9.49	22.52	98.89	210.63	122.56	19.59	8.11	4.84

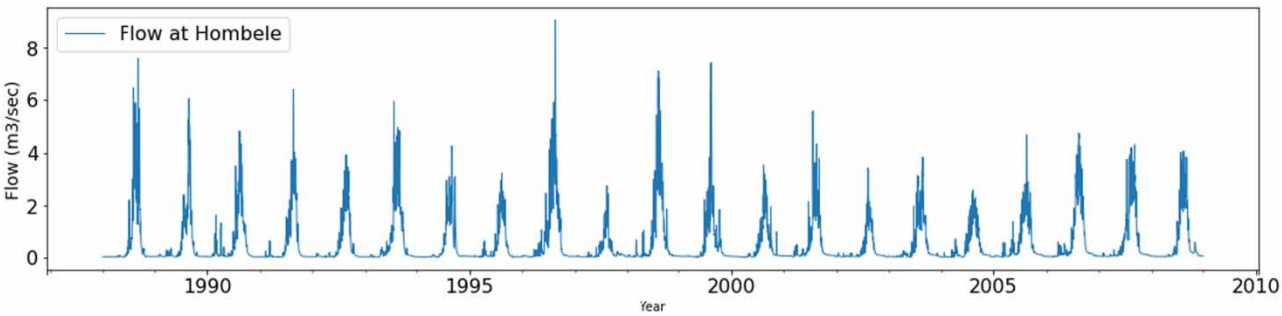

Figure 4 | Annual flow at the Hombele station.

Table 3 | Average monthly and annual precipitation of Hombele catchment

Station Name	Jan	Feb	Mar	Apr	May	Jun	Jul	Aug	Sep	Oct	Nov	Dec	Annual
AAO	12.80	34.00	63.60	89.44	78.85	141.46	272.61	293.64	179.21	36.70	9.76	9.30	1,221.39
Akaki	11.20	27.77	56.06	88.41	63.00	109.45	237.51	243.26	117.52	18.97	5.51	5.58	984.24
Asgori	17.57	28.22	65.51	86.77	69.95	145.15	240.74	235.87	108.14	18.92	9.15	4.83	1,030.81
Bantu Liben	15.24	18.25	61.72	85.34	75.50	176.31	309.96	308.22	149.08	36.74	13.89	7.60	1,257.85
Boneya	7.01	26.29	44.73	66.38	62.97	114.57	204.70	219.02	110.41	12.31	6.90	5.59	880.88
Enselale	11.88	23.93	40.73	63.61	47.44	113.09	193.34	177.69	90.15	18.47	6.21	5.85	792.39
Ginchi	26.71	42.09	74.13	95.78	85.52	154.39	231.88	250.10	146.20	39.60	10.89	10.99	1,168.28
Dertu Liben	12.43	29.04	42.67	74.85	45.08	94.85	185.89	166.53	86.31	24.06	4.79	7.81	774.32
Holetta	27.1	46.2	62.7	84.5	66.6	110.6	243.7	263.2	129.6	14.9	6	9.4	1,064.50
Sebeta	15	53.2	76.7	94.2	95.3	168	305.9	336.1	133.3	34.7	7.5	6.7	1,326.60
Teji	12.69	29.75	54.35	75.77	69.94	131.59	218.20	220.33	99.75	19.76	6.69	6.41	945.23
Tulobolo	11.30	13.47	43.52	66.31	96.86	225.56	282.84	284.62	114.66	19.17	3.48	5.64	1,167.42
Addis Alem	15.16	35.63	70.81	60.05	82.16	143.43	263.02	238.32	131.16	30.26	23.82	13.37	1,107.18
Sendafa	14.63	22.60	41.06	79.24	47.33	113.10	322.76	313.85	106.39	18.27	4.35	3.39	1,086.97

Table 4 | Monthly mean maximum and minimum temperatures at selected stations

	Addis Ababa		Debre Zeit		Holeta	
Month	Mean max temp. (°C)	Mean min temp. (°C)	Mean max temp. (°C)	Mean max temp. (°C)	Mean max temp. (°C)	Mean max temp. (°C)
Jan	17.47	12.78	19.68	17.19	23.1	13.2
Feb	18.33	14.01	20.98	18.43	23.8	15.2
Mar	23.2	15.19	21.8	19	24.2	14.1
Apr	19.33	16.39	22.61	19.21	23.7	16.2
May	19.4	16.14	22.58	19.76	24.2	11.9
Jun	19.04	15.52	21.66	18.93	22.1	12
Jul	17.12	14.57	20.54	18.42	19.8	10
Aug	17.07	14.46	19.6	18.12	19.2	10
Sep	16.97	13.99	20.09	17.89	20.2	11.2
Oct	17.26	13.04	20.05	16.36	21.6	12.3
Nov	16.1	11.94	19.07	16.13	22.3	12.8
Dec	16.65	12.17	19.45	14.88	22.9	13.2

2.4. Model setup

To investigate the suitability of groundwater recharge under different levels of complexity of the model, the HBV-light model was run with two levels of complexity and five objective functions. In the first configuration of HBV-light (semi-distributed), the study catchment area was divided into nine altitude zones with a vertical distance of 200 m (Figure 5), and orographic effects on precipitation and temperature were taken into account. In the configuration of the second model (lumped), only one altitude zone was considered in the study area, and the influence of orography on precipitation and temperature was excluded. The mean height of each zone was calculated from a 30 m × 30 m digital elevation model.

2.5. Calibration, validation, and sensitivity

In this study, groundwater recharge model calibration was applied for both levels of model complexity and model objective functions. The Nash–Sutcliffe efficiency (NSE) was used as the objective function in the MC-based calibration approach to adjust nine HBV-light model parameters (Table 1). The HBV-light model runs for 10,000, and therefore the best parameter sets (1,000 from 10,000 parameter sets) were selected based on the NSE value, 0.6. Among the 1,000 parameter sets, a single parameter set with the highest NSE value was applied to simulate groundwater recharge. However, it is vital to notice that the

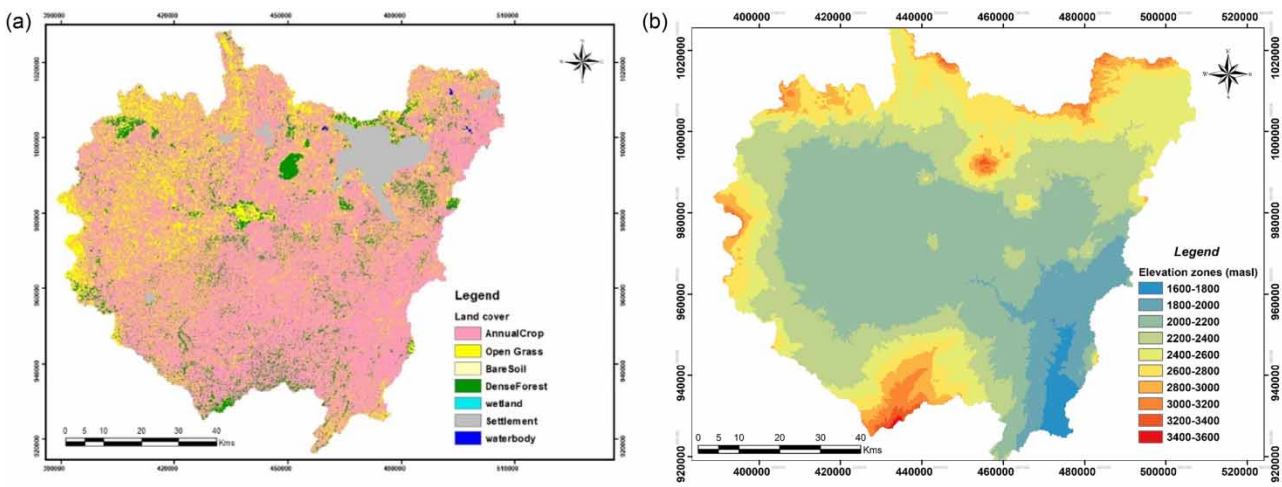

Figure 5 | The study catchment's land cover map (a) (source: Ethiopian Geospatial Agency) and the elevation zones (b).

hydrological model calibration employing a single fine-tuned parameter set results in equifinality (Uhlenbrook & Leibundgut 1999; Choi & Beven 2007), which is not taken under consideration within the current study. The HBV-light model was calibrated for the period 1986–2008 during which 1986–1987 is a warm-up period. The model validation was employed from 2009 through 2013 using independent datasets.

The one-factor-at-a-time (OAT) method was used to analyze the sensitivity of the model parameters for different combinations of precipitation inputs and model complexity. Several studies that examined sensitivity analysis have made extensive use of this methodology (van Griensven *et al.* 2006; Nonki *et al.* 2021). To perform OAT, the model was run 1,000 times, varying one parameter while keeping the other parameters constant. The value of the best-fit parameter of the MC simulation and the corresponding range of values (Table 1) were used to perform the OAT. Based on the different objective functions such as Kling–Gupta efficiency (KGE), NSE, coefficient of determination (R^2), LogNSE, and Volume Error (VE), the most influential parameters that have a strong influence on the model simulation result were identified and then refined to improve the efficiency of the model.

2.6. Model performance evaluation

In this study, the suitability of groundwater recharge estimation for different levels of model complexity was evaluated using five performance metrics: NSE, KGE, percentage of bias (PBIAS), R^2, and volumetric efficiency. The NSE (Equation (5)) is a normalized statistic that assesses the proportion of residual variance (also known as 'noise') to measured data variance (also known as 'information') (Sutcliffe 1970). NSE range from −Inf to 1. In general, the model is more accurate the closer it is to 1. NSE = 1 implies that the model and observed data are perfectly matched, NSE = 0 implies that the model's predictions are as accurate as the observed data's mean, and −Inf < NSE < 0 implies that the observed mean is a better predictor than the model. A negative value indicates the poor performance of the model.

$$\mathrm{NSE} = 1 - \frac{\sum_{i=1}^{N} (S_i - O_i)^2}{\sum_{i=1}^{N} (O_i - \bar{o})^2} \tag{5}$$

KGE (Equation (6)) was developed by Gupta *et al.* (2008) to provide an interesting diagnostic decomposition of the NSE, which facilitates the analysis of the relative importance of its various components (correlation, bias, and variability) in the context of hydrological modeling. The optimal value of KGE is 1.0. The KGE metric was also used to compare the recharge estimates for different rainfall-forcing datasets once an optimal model complexity setup was identified for the study catchment.

$$\mathrm{KGE} = 1 - \sqrt{(r-1)^2 + (\beta - 1)^2 + (\gamma - 1)^2} \tag{6}$$

where r is the linear correlation coefficient between the simulated and observed value, $\beta =$, $\gamma = (\delta_S/\delta_O)$ μ_s and μ_o are the mean simulated and observed value, and δ_S and δ_O are the standard deviations of the simulated and observed values, respectively.

PBIAS is a measure of the average tendency for the simulated values to differ from their observed values in either a larger or smaller manner (Equation (7)). Low values of PBIAS signify accurate model simulation, and the value should be set to 0. While negative values indicate an underestimation of the model, positive numbers indicate an overestimation bias (Gupta *et al.* 1999).

$$\mathrm{PBIAS} = 100 \frac{\sum_{i=1}^{N} (S_i - O_i)}{\sum_{i=1}^{N} O_i} \tag{7}$$

R^2 (Equation (8)) measures the performance model to predict the observed values in a linear regression configuration. Its value ranges from 0.0 to 1.0, and the higher the R^2 value the better the model fit.

$$R^2 = \frac{\left[\sum_{i=1}^{N} (O - \bar{O})(S_i - \bar{S})\right]^2}{\sum_{i=1}^{N} (O_i - \bar{O})^2 \sum_{i=1}^{N} (S_i - \bar{S})^2}. \tag{8}$$

The VE was suggested (Equation (9)) to get around some issues with the NSE. It reflects the portion of water provided at the appropriate moment and runs from 0 to 1; its counterpart denotes the fractional volumetric mismatch (Criss & Winston 2008).

$$\mathrm{VE} = 1 - \frac{\sum_{i=1}^{N} |S_i - O_i|}{\sum_{i=1}^{N} (O_i)} \tag{9}$$

where N is the number of compared values, O_i are the observed values, O^- are the mean observed values, and S_i are the simulated values.

The hydrograph and scatter plot were used to compare the observed and simulated flows in addition to these statistical evaluation criteria. The model that performed the best in simulating recharge estimation was selected based on statistical evaluation metrics.

3. RESULTS AND DISCUSSION

3.1. Sensitivity of HBV-light model parameters under different levels of model complexity and objective function

We conducted a sensitivity analysis of the HBV-light model parameters to evaluate how the sensitivity of these parameters is affected by varying levels of model complexities and objective functions. The results are shown in Figure 5 and indicate that both the objective function and model complexity can influence the sensitivity of the HBV-light model parameters. When analyzing the HBV-light model as a semi-distributed one, it was found that the FC and BETA parameters showed the highest level of sensitivity when using the R^2 and KGE objective functions. In addition, when the NSE objective function was utilized, the FC and LP parameters were found to be the most sensitive. In contrast, PERC, UZL, K0, K1, and MAXBAS parameters were observed to be less sensitive across all objective functions. In Figure 6, when the HBV-light model was used as a lumped model, it was discovered that the FC, LP, and BETA parameters were the most sensitive across all three objective functions. On the other hand, parameters UZL, K0, and MAXBAS were less sensitive in this model configuration. In addition, it was noted that the NSE objective function had a higher sensitivity compared to the KGE and VE objective functions at both levels of model complexity.

In this study, a sensitivity analysis was performed to determine the impact of various model parameters on the flow within the catchment area. The results indicated that the FC, LP, and BETA parameters had the greatest sensitivity across different objective functions and model complexities. These parameters were found to significantly affect the simulation of flow. On the other hand, the UZL, K0, and MAXBAS parameters had minimal influence on the model results. The results underscore the significant impact of the objective function and model complexity on parameter sensitivity. Specifically, when using the VE objective function, FC, LP, and MAXBAS consistently emerged as the most sensitive parameters across both model complexities. Conversely, PERC, UZL, K0, K1, and MAXBAS showed minimal levels of influence. When analyzing the LogNSE objective function, it was found that the semi-distributed HBV-light model was most sensitive to the K2 parameter. On the other hand, the lumped model complexity showed that BETA and PERC were the most influential parameters. It is worth noting that the sensitivity of the model parameters is greatly influenced by the methods used to conduct the sensitivity analysis (Devak & Dhanya 2017) and the objective functions chosen (Nonki *et al.* 2021).

3.2. Model calibration and validation

During the calibration and validation processes, we tested various combinations of model complexities and objective functions to evaluate the performance of the model. In general, the model performed well in replicating the observed flow, as evidenced by the highest scores of objective functions. However, there were certain inconsistencies between the simulated and observed flows, particularly in accurately capturing the peak discharge events. When analyzing the semi-distributed model's complexity, it was found that the model underestimated the peak discharge when using objective functions like KGE and NSE. This suggests that the peak discharge values obtained from simulation were lower than the observed values. On the other hand, when using objective functions like R^2 and VE, the model tended to overestimate the peak discharge, with simulated values surpassing the observed values. We noticed similar trends in the complexity of the lumped model. When using objective functions like KGE, NSE, and VE, the peak discharge was often underestimated. However, this underestimation was not consistently observed when using other objective functions. There are several factors that

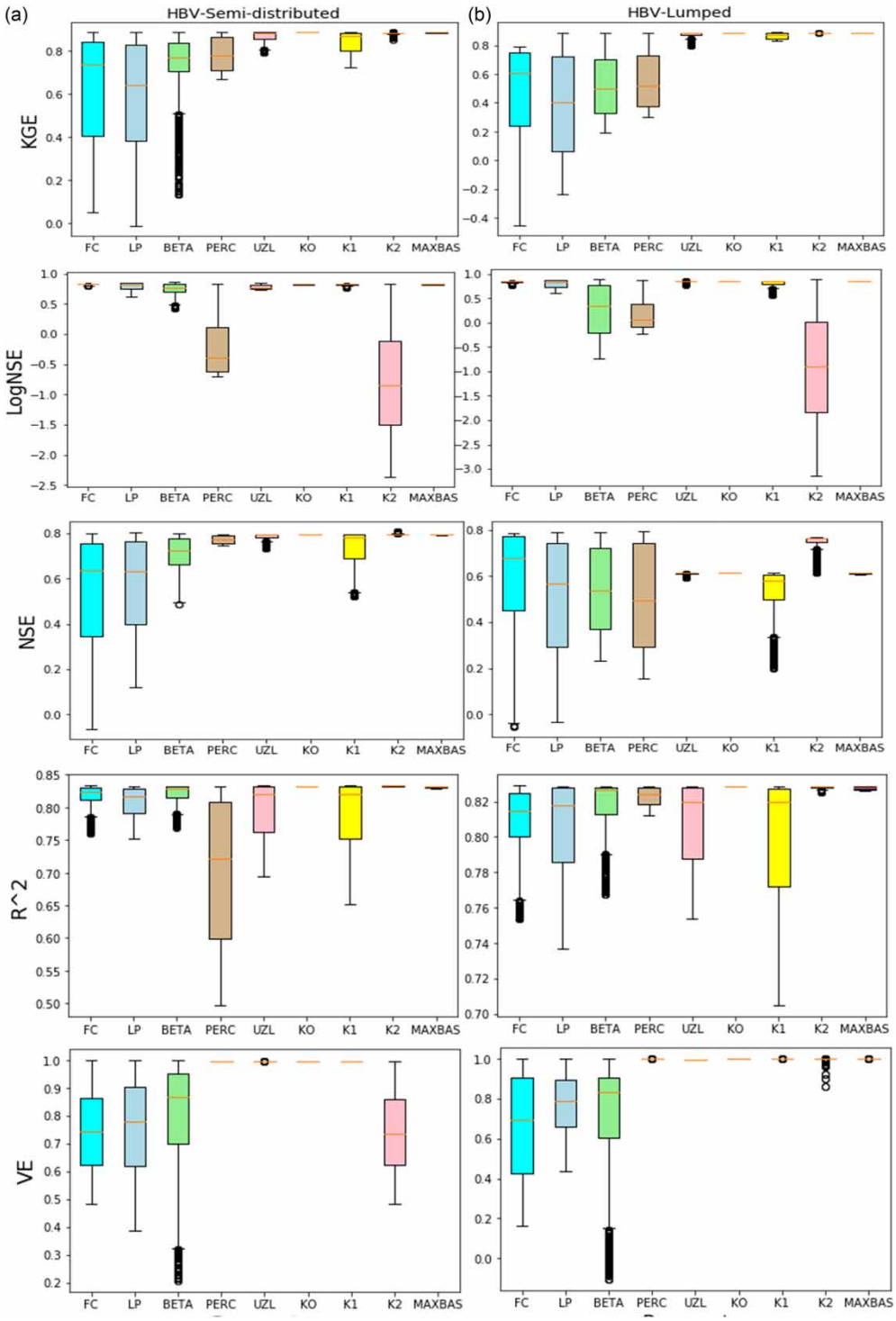

Figure 6 | Boxplots showing the sensitivity of model parameters for different objective functions and model complexities (semi-distributed and lumped). The middle horizontal line of the box plot shows the median values, whereas the top and bottom lines indicate the 75th and 25th percentiles, respectively.

can contribute to the underestimation or overestimation of peak discharge in a model. These factors include the complexity of the model, the choice of objective functions, the sensitivity of model parameters, and limitations in the available data as shown in Figure 7.

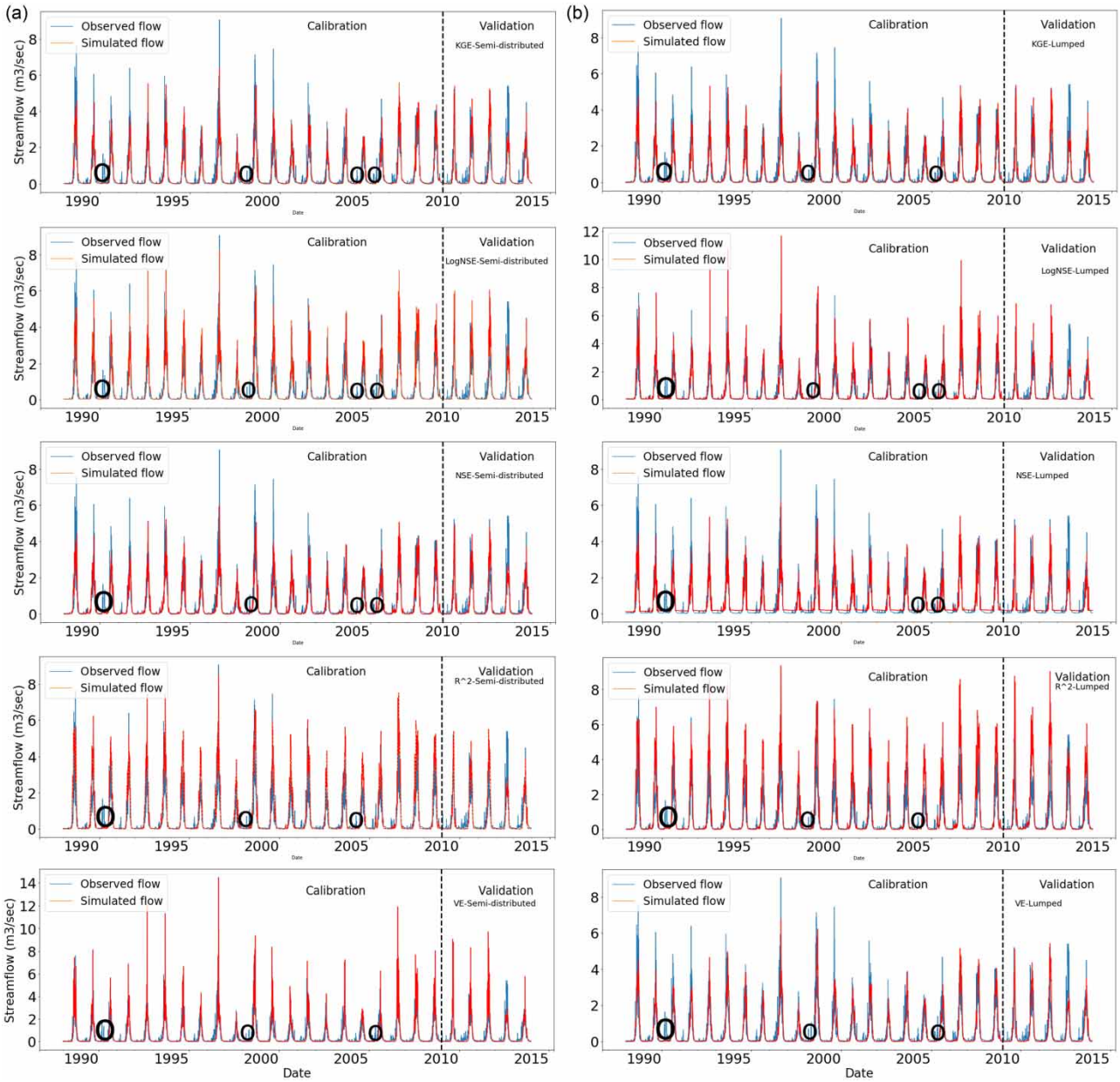

Figure 7 | Comparison of daily observed and simulated streamflow of the Hombele gauging station during 1 January 1988 to 31 December 2008 for calibration and 1 January 2009 to 31 December 2013 for validation for semi-distributed (a) and lumped (b) for different objective functions.

Figure 7 shows the comparison of daily observed and simulated streamflow from the Hombele gauging station during the period 1 January 1988 to 31 December 2008 for calibration and 1 January 2009 to 31 December 2013 for validation for semi-distributed (a) and lumped (b) and different objective functions. We noticed errors in the streamflow measurements, which are highlighted by black circles. We provided two reasons for detecting these errors. The first reason is that in some cases, streamflow measurements were recorded even when all available rainfall inputs indicated no rainfall. This suggests that there may be observational errors in the data. It is possible that there were mistakes or inaccuracies in the process of measuring and recording streamflow, leading to these discrepancies. The second reason is related to the baseflow component, which represents the contribution of groundwater to streamflow. We noted that this component had a relatively minor impact on the daily streamflow values. This observation suggests that there may be inconsistencies in the observed data, which can affect the

accuracy of the model's performance. During the calibration period, the model exhibited superior performance regardless of the combination of objective functions and model complexities. This indicates that an acceptable fit was achieved by the model's ability to calibrate its parameters to match the observed data. We did note, however, that the model's precision throughout the validation period might be lower. This is because the model is evaluated using independent data that were not used for calibration. Therefore, any discrepancies or errors in the observed data during the validation period may lead to less accurate model performance.

The findings of assessing the performance of the semi-distributed and the lumped HBV-light model in combination with the KGE objective function are shown in the following statement. The outcomes indicate the calibration scores for multiple metrics, such as R^2, NSE, PBIAS, KGE, and VE. The semi-distributed HBV model had calibration scores of $R^2 = 0.79$, NSE = 0.78, PBIAS = −0.3, KGE = 0.89, and VE = 0.59. The lumped HBV-light model had calibration scores of $R^2 = 0.77$, NSE = 0.76, PBIAS = −1.5, KGE = 0.88, and VE = 0.58. These evaluations show the degree of agreement between the observed data and the model-generated simulated data.

The LogNSE objective function combined with the semi-distributed and lumped HBV-light model produced the best results during model calibration. The calibration score, as measured by the R^2, was 0.8 (0.8), indicating a strong correlation between the observed and simulated values. The NSE score was also high at 0.79 (0.77), showing a good fit between the observed and simulated values. In contrast, the use of other performance evaluation matrices, such as KGE and PBIAS, resulted in lower model performance, particularly for the lumped model complexity levels. This suggests that these objective functions were not as effective in accurately determining the model's performance.

The combination of the NSE objective function and the semi-distributed HBV-light model produces better results compared to the lumped HBV-light model. The semi-distributed and lumped model yielded a better calibration score with an NSE of 0.8 (0.73) and a KGE of 0.88 (0.81), respectively. It is worth noting that both models performed well despite their different complexity levels. The semi-distributed model, which accounts for spatial variability in the watershed, outperformed the lumped model in terms of calibration score and overall performance. However, the lumped model, which assumes uniform characteristics throughout the watershed, still provided a reasonably accurate representation of the system.

When the objective functions VE and R^2 were used, the model's performance was lower for both model complexity levels than the other objective functions. This indicates that these objective functions were less effective in evaluating the model's accuracy. Figure 8 illustrates the linear correlation between the observed and simulated flows, which offers valuable information on the model's capacity to capture changes in streamflow.

3.3. Estimating groundwater recharge for different levels of model complexity and objective functions

By utilizing the MC calibration approach to determine the optimal model parameters, we were able to estimate groundwater recharge through the use of five objective functions and five evaluation matrices. Our findings indicated that recharge levels throughout the study area were dependent on the particular model configuration being utilized (Table 5). The recharge values for the semi-distributed HBV-light model ranged from 185.9 to 280.5 mm. On the other hand, the recharge values for the lumped HBV-light model ranged from 185.3 to 321.7 mm. These variations indicate that the model configuration has a significant impact on the estimated recharge values (Table 6 and Figure 8). In the study area, the recharge rate for the semi-distributed model was estimated to be 196.9 mm when the NSE objective function was utilized. However, when the KGE objective function was used, the recharge rate was estimated to be 185.9 mm. These findings emphasize the significance of the chosen objective function in determining the estimated recharge. To determine the most effective method for estimating groundwater recharge, various objective functions were evaluated. The objective functions with the highest NSE, KGE, R^2, VE, and lowest PBIAS values were identified as the most suitable options for estimating groundwater recharge, regardless of the complexity level of the model (Table 7). Figure 9 displays the graphical representation of annual groundwater recharge for two different model complexities and objective functions. In general, analyzing groundwater recharge through the use of different objective functions and evaluation matrices can offer useful information on recharge patterns in a particular area. The findings highlight the significance of selecting the right objective functions and model configurations to achieve precise estimates of groundwater recharge.

4. SUMMARY AND CONCLUSION

The study utilized the HBV-light model to determine the amount of groundwater recharge in the Hombele catchment, situated in the Upper Awash basin in Ethiopia. The objective was to compare the outcomes of groundwater recharge estimations

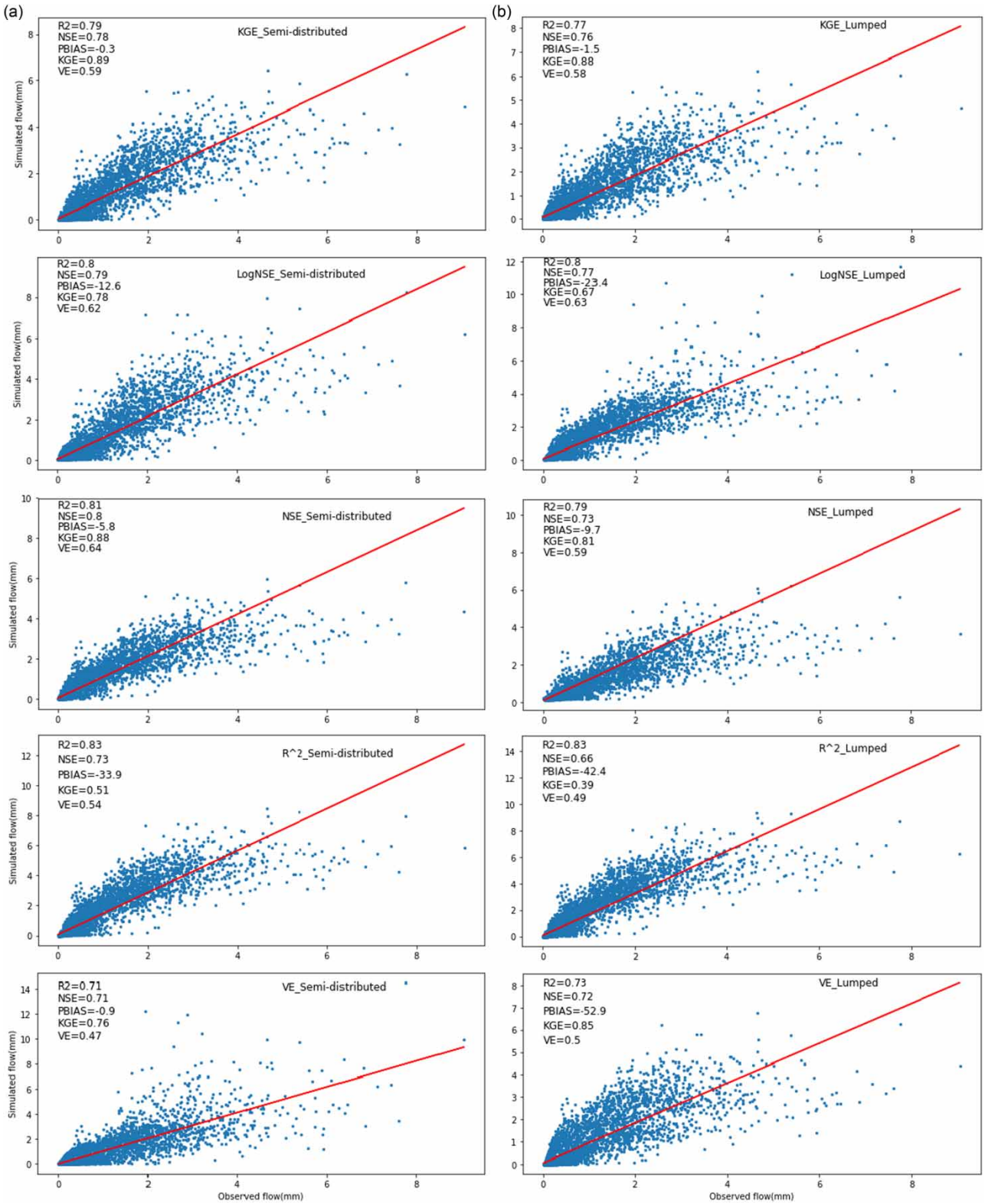

Figure 8 | Scatter plot of daily simulated and observed discharge during the calibration of semi-distributed and lumped for different objective functions.

Table 5 | Optimized model parameters for different objective functions and model complexities

	NSE	KGE	R^2	LogNSE	VE
FC	529.1 (503.8)	436.48 (464.9)	366.38 (338.01)	464.41 (508.66)	296.72 (478.9)
LP	0.368 (0.302)	0.41 (0.32)	0.98 (0.96)	0.66 (0.744)	0.34 (0.613)
BETA	1.85 (1.53)	2.69 (1.96)	4.53 (3.381)	3.11 (2.56)	4.98 (3.27)
PERC	0.195 (0.59)	0.35 (0.78)	0.04 (0.054)	0.08 (0.14)	1.78 (0.42)
UZL	62.92 (67.84)	46.96 (69.6)	68.3 (65.46)	15.17 (28.18)	8.91 (46.41)
K0	0.162 (0.134)	0.25 (0.33)	0.46 (0.176)	0.17 (0.42)	0.46 (0.102)
K1	0.159 (0.19)	0.15 (0.15)	0.15 (0.151)	0.05 (0.137)	0.16 (0.093)
K2	0.076 (0.00077)	0.03 (0.053)	0.014 (0.075)	0.002 (0.003)	0. 07(0.096)
MAXBAS	1.47 (2.153)	1.098 (1.16)	1.72 (1.92)	1.26 (2.12)	1.48 (1.026)

Note: The value inside the bracket indicates the best-fitted parameter value for lumped model complexity.

Table 6 | Groundwater recharge for the different objective functions and two model complexities

	Model complexity			
	Semi-distributed		Lumped	
Objective function	Recharge (mm/year)	% of recharge	Recharge (mm/year)	% of recharge
NSE	196.9	18.5	211.2	19.9
KGE	185.9	17.5	188.1	17.7
R2	280.5	26.4	185.3	17.4
LogNSE	211.7	19.9	321.7	30.3
VE	187	17.6	241.8	22.8
Average	**212.4**	**20.0**	**229.6**	**21.6**

Table 7 | The performance of the HBV-light model in simulating streamflow for different combinations of objective functions and model complexity during the calibration (1988–2008), validation (2009–2013), and full (1988–2013) periods

		Calibration period					Validation period					Full period				
Model complexity	Objective function	NSE	KGE	R^2	PBIAS	VE	NSE	KGE	R^2	PBIAS	VE	NSE	KGE	R^2	PBIAS	VE
Semi-distributed	KGE	0.78	0.89	0.79	−0.3	0.59	0.7	0.8	0.7	0.1	0.5	0.76	0.87	0.8	−0.1	0.6
	NSE	0.8	0.88	0.81	−5.8	0.64	0.73	0.83	0.73	−0.1	0.55	0.77	0.89	0.8	−0.4	0.6
	LogNSE	0.79	0.78	0.8	−12.6	0.62	0.67	0.77	0.67	−0.1	0.5	0.75	0.85	0.8	−0.8	0.6
	R^2	0.73	0.51	0.83	−33.9	0.54	0.7	0.76	0.7	0.1	0.45	0.77	0.84	0.8	−0.3	0.5
	VE	0.71	0.76	0.71	−0.9	0.47	0.6	0.68	0.6	0.9	0.38	0.68	0.76	0.7	0.8	0.5
Lumped	KGE	0.76	0.88	0.77	−1.5	0.58	0.69	0.8	0.69	0.3	0.49	0.73	0.86	0.8	0.1	0.6
	NSE	0.73	0.81	0.79	−9.7	0.59	0.63	0.8	0.67	−0.5	0.52	0.63	0.76	0.7	0.6	0.5
	LogNSE	0.77	0.67	0.8	−23.4	0.63	0.67	0.79	0.67	0.3	0.53	0.73	0.86	0.7	−0.4	0.6
	R^2	0.66	0.39	0.83	−42.4	0.49	0.57	0.33	0.75	−44.5	0.45	0.67	0.36	0.8	−44.6	0.5
	VE	0.72	0.85	0.73	−52.9	0.5	0.64	0.76	0.64	−0.2	0.41	0.7	0.83	0.7	−0.6	0.5

by varying the model complexity and objective functions. Two levels of model complexities were considered in this study. The first level, known as semi-distributed model complexity, involves dividing the study area into nine elevation zones with a vertical spacing of 200 m. This allowed for consideration of orographic effects on rainfall and temperature. The second level, referred to as lumped model complexity, focuses on only one elevation zone and ignores orographic effects. A MC calibration

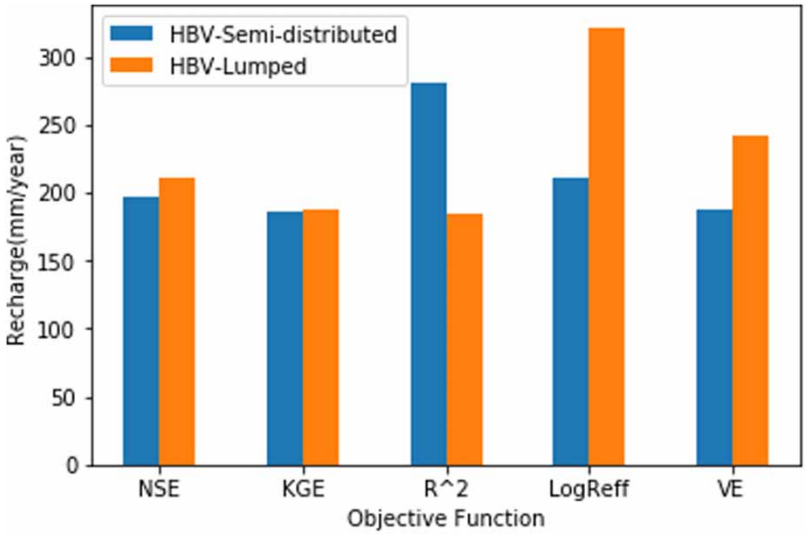

Figure 9 | Annual groundwater recharge for two model complexities and different objective functions.

scheme was employed to calibrate the model parameters. The calibration process aimed to find the best-fit parameters for each rainfall input, with the NSE objective function. Using this scheme, the model parameters were adjusted to better match the observed data. To evaluate how well the model estimates groundwater recharge, we used five different objective functions: NSE, KGE, PBIAS, R^2, and VE. By using these performance metrics, we were able to thoroughly assess the model's ability to simulate the groundwater recharge rate across various objective functions. The main objective of this study was to determine the most effective approach for estimating the groundwater recharge rate in the Hombele catchment. This was done by comparing the results obtained from various combinations of model complexities and objective functions. The analysis provided valuable insights into the reliability and accuracy of the HBV-light model in this specific context.

- Model objective functions and model complexities have a significant impact on the sensitivity of the HBV-light model parameters and objective functions.
- In most of the objective functions, the FC and LP parameters are the most sensitive model parameters when using the HBV-light model as a lumped and a semi-distributed one. MAXBAS and K0 are noninfluential model parameters in the study catchment for both model complexity and all objective functions.
- Better calibration and validation results were obtained when using a semi-distributed HBV-light model with NSE and KGE objective functions.
- The model-based recharge estimation depends on the objective function used and the levels of model complexity.
- The groundwater recharge rates in the study region range from 185.9 to 280.5 mm/year when using a semi-distributed HBV-light model and from 185.3 to 321.7 mm/year for a lumped HBV-light model.

The available data collected onsite is limited in quantity and unevenly distributed across the study area. In addition, there may be uncertainties associated with the accuracy and reliability of the observations.

To enhance the quality of this study, it is essential to establish monitoring stations capable of collecting a diverse range of climate and hydrological data. These stations should be equipped with instruments that can measure variables such as stream flow, rainfall, and temperature.

Conducting field studies and collecting comprehensive and accurate data on groundwater recharge is essential for validating and improving the results of the model used in this study. These efforts contribute to a better understanding of the hydrological processes in the study region and enhance the reliability of the study's findings and recommendations.

Overall, it is important to consider the uncertainty of model complexity and objective function while quantifying the major water balance components of the study region.

ACKNOWLEDGEMENTS

Dr. Seifu Kebede was unable to verify their authorship due to unforeseen reasons, however the Corresponding Author is able to vouch for their authorship and the Author contributed as an advisor in the Ph.D fellowship of the Corresponding Author.

DATA AVAILABILITY STATEMENT

All relevant data are included in the paper or its Supplementary Information.

CONFLICT OF INTEREST

The authors declare there is no conflict.

REFERENCES

Allan, R., Pereira, L. & Smith, M. 1998 Crop evapotranspiration – Guidelines for computing crop water requirements – FAO Irrigation and drainage, paper 56.

Azagegn, T. 2014 *Groundwater Dynamics in the Left Bank Catchments of the Middle Blue Nile and the Upper Awash River Basins*. PhD Thesis.

Baye, A. Y. 2009 *Hydrogeological and Hydrochemical Framework of Complex Volcanic System in the Upper Awash River Basin, Central Ethiopia: With Special Emphasis on Inter-Basins Groundwater Transfer Between Blue Nile and Awash*. PhD Thesis.

Baye, A., Razack, M., Ayenew, T. & Zemedagegnehu, E. 2012 Estimating transmissivity using empirical and geostatistical methods in the volcanic aquifers of Upper Awash Basin, central Ethiopia. *Environ. Earth Sci.* **69**. https://doi.org/10.1007/s12665-012-2011-6.

Berehanu, B., Azagegn, T., Ayenew, T. & Masetti, M. 2017 Inter-basin groundwater transfer and multiple approach recharge estimation of the upper awash aquifer system. *J. Geosci. Environ. Prot.* **05**, 76–98. https://doi.org/10.4236/gep.2017.53007.

Bergstrom, S. 1991 Principles and confidence in hydrological modelling. *Nord. Hydrol.* **22**, 123–136. https://doi.org/10.2166/nh.1991.0009.

Bergström, S. 2006 Experience from applications of the HBV hydrological model from the perspective of prediction in ungauged basins. *IAHS-AISH Publ.* 97–107.

Birhanu, B., Kebede, S., Masetti, M. & Ayenew, T. 2018 WEAP-MODFLOW dynamic modeling approach to evaluate surface water and groundwater supply sources of Addis Ababa city. *Acque Sotter. Ital. J. Groundw.* **7**, 15–24. https://doi.org/10.7343/as-2018-334.

Choi, H. T. & Beven, K. 2007 Multi-period and multi-criteria model conditioning to reduce prediction uncertainty in an application of TOPMODEL within the GLUE framework. *J. Hydrol.* https://doi.org/10.1016/j.jhydrol.2006.07.012.

Criss, R. E. & Winston, W. E. 2008 Do Nash values have value? Discussion and alternate proposals. *Hydrol. Process.* **22**, 2723–2725. https://doi.org/10.1002/hyp.7072.

Dassi, L. 2010 Use of chloride mass balance and tritium data for estimation of groundwater recharge and renewal rate in an unconfined aquifer from North Africa: A case study from Tunisia. *Environ. Earth Sci.* **60**, 861–871. https://doi.org/10.1007/s12665-009-0223-1.

Devak, M. & Dhanya, C. T. 2017 Sensitivity analysis of hydrological models: Review and way forward. *J. Water Clim. Chang.* **8**, 557–575. https://doi.org/10.2166/wcc.2017.149.

Gidafie, D., Tafesse, N. & Hagos, M. 2016 Estimation of groundwater recharge using water balance model: A case study in the Gerado basin, North Central Ethiopia. *IJEE* **9**, 942–950.

Gupta, H. V., Sorooshian, S. & Ogou, P. 1999 Status of automatic calibration for hydrologic models: Comparison with multilevel expert calibration. *J. Hydrol. Eng.* **4**, 135–143.

Gupta, H., Wagener, T. & Liu, Y. 2008 Reconciling theory with observations: Elements of a diagnostic approach to model evaluation. *Hydrol. Process.* **22**, 3802–3813. https://doi.org/10.1002/hyp.6989.

Healy, R. W. & Cook, P. G. 2002 Using groundwater levels to estimate recharge. *Hydrogeol. J.* **10**, 91–109. https://doi.org/10.1007/s10040-001-0178-0.

Izady, A., Abdalla, O. A. E., Joodavi, A., Karimi, A., Chen, M. & Tompson, A. 2017 Groundwater recharge estimation in arid hardrock-alluvium aquifers using combined water-table fluctuation and groundwater balance approaches. *Hydrol. Process.* **31**, 3437–3451. https://doi.org/10.1002/hyp.11270.

Kidanewold, B., Seleshi, Y. & Melesse, A. 2014 Surface water and groundwater resources of Ethiopia: potentials and challenges of water resources development. In: *Nile River Basin: Ecohydrological Challenges, Climate Change and Hydropolitics*, pp. 97–118. https://doi.org/10.1007/978-3-319-02720-3_6.

Li, Z., Chen, X., Liu, W. & Si, B. 2017 Determination of groundwater recharge mechanism in the deep loessial unsaturated zone by environmental tracers. *Sci. Total Environ.* **586**, 827–835. https://doi.org/10.1016/j.scitotenv.2017.02.061.

MacDonald, A. M., Lark, R. M., Taylor, R. G., Abiye, T., Fallas, H. C., Favreau, G., Goni, I. B., Kebede, S., Scanlon, B., Sorensen, J. P. R., Tijani, M., Upton, K. A. & West, C. 2021 Mapping groundwater recharge in Africa from ground observations and implications for water security. *Environ. Res. Lett.* **16**. https://doi.org/10.1088/1748-9326/abd661.

Mechal, A., Wagner, T. & Birk, S. 2015 Recharge variability and sensitivity to climate: The example of Gidabo River Basin, Main Ethiopian Rift. *J. Hydrol. Reg. Stud.* **4**, 644–660. https://doi.org/10.1016/j.ejrh.2015.09.001.

Neil, G. O., 2015 Mapping Groundwater Recharge Rates Under Multiple Future Climate Scenarios in Southwest Michigan, pp. 1–39. https://swat.tamu.edu/media/115033/k1_3_oneil.pdf.

Nonki, R. M., Lenouo, A., Tshimanga, R. M., Donfack, F. C. & Tchawoua, C. 2021 Performance assessment and uncertainty prediction of a daily time-step HBV-light rainfall-runoff model for the Upper Benue River Basin, Northern Cameroon. *J. Hydrol. Reg. Stud.* **36**. https://doi.org/10.1016/j.ejrh.2021.100849.

Parlov, J., Kovač, Z., Nakić, Z. & Barešić, J. 2019 Using water stable isotopes for identifying groundwater recharge sources of the unconfined alluvial Zagreb aquifer (Croatia). *Water (Switzerland)* **11**. https://doi.org/10.3390/w11102177.

Scanlon, B. R., Healy, R. W. & Cook, P. G. 2002 Choosing appropriate techniques for quantifying groundwater recharge. *Hydrogeol. J.* **10**, 18–39. https://doi.org/10.1007/s10040-001-0176-2.

Scanlon, B., Keese, K., Flint, A., Flint, L., Gaye, C. B., Edmunds, W. & Simmers, I. 2006 Global synthesis of groundwater recharge in semiarid and arid regions. *Hydrol. Process.* **20**, 3335–3370. https://doi.org/10.1002/hyp.6335.

Seibert, J. 1997 Estimation of parameter uncertainty in the HBV model. *Nord. Hydrol.* **28**, 247–262. https://doi.org/10.2166/nh.1998.15.

Seibert, J. 2000 Multi-criteria calibration of a conceptual runoff model using a genetic algorithm. *Hydrol. Earth Syst. Sci.* **4** (2), 215–224.

Seleshi, Y. & Zanke, U. 2004 Recent changes in rainfall and rainy days in Ethiopia. *Int. J. Climatol.* **24**, 973–983. https://doi.org/10.1002/joc.1052.

Sutcliffe, N. 1970 River flow forecasting through conceptual models part I – A discussion of principles. *J. Hydrol.* **10**, 282–290.

Tenalem, A. 2019 Comparison of different base flow separation methods and drought vulnerability in a rift valley area. *J. Spat. Hydrol.* **15**, 1–27.

Uhlenbrook, S. & Leibundgut, C. 1999 Integration of tracer information into the development of a rainfall-runoff model. *IAHS-AISH Publ.* **258**, 93–100.

van Griensven, A., Meixner, T., Grunwald, S., Bishop, T., Diluzio, M. & Srinivasan, R. 2006 A global sensitivity analysis tool for the parameters of multi-variable catchment models. *J. Hydrol.* **324**, 10–23. https://doi.org/10.1016/j.jhydrol.2005.09.008.

Varouchakis, E., Kalaitzaki, E., Trichakis, I., Corzo, G. & Karatzas, G. 2022 An integrated method to study and plan aquifer recharge. *Hydrol. Res.* **54**. https://doi.org/10.2166/nh.2022.054.

Verma, K., Manisha, M., Santrupt, R. M., Anirudha, T. P., Goswami, S., Sekhar, M., Ramesh, N., Sekhar, M. K., Chanakya, H. N. & Rao, L. 2023 Assessing groundwater recharge rates, water quality changes, and agricultural impacts of large-scale water recycling. *Sci. Total Environ.* **877**, 162869. https://doi.org/10.1016/j.scitotenv.2023.162869.

Yun, S.-M., Jeon, H.-T., Cheong, J.-Y., Kim, J. & Hamm, S.-Y. 2023 Combined analysis of net groundwater recharge using water budget and climate change scenarios. *Water* **15**, 571. https://doi.org/10.3390/w15030571.

Zinko, U., Seibert, J., Dynesius, M. & Nilsson, C. 2005 Plant species numbers predicted by a topography-based groundwater flow index. *Ecosystems* **8**, 430–441. https://doi.org/10.1007/s10021-003-0125-0.

First received 26 April 2023; accepted in revised form 19 January 2024. Available online 1 February 2024